ARTICLE

Nanocarbon-Induced Rapid Transformation of Polymer Surfaces into Superhydrophobic Surfaces

Joong Tark Han,*,† Jun Suk Kim,† Seong Hoon Kim,† Ho Sun Lim,‡ Hee Jin Jeong,† Seung Yol Jeong,† and Geon-Woong Lee*,†

Nano Carbon Materials Research Group, Korea Electrotechnology Research Institute, Changwon 641-120, Korea, and Department of Materials Science and Engineering, Institute for Soldier Nanotechnologies, Massachusetts Institute of Technology, Cambridge, Massachusetts 02139, United States

ABSTRACT We present a facile method for fabricating superhydrophobic polymer surfaces by solubility modulation and nanocarbon (NC)-induced crystallization of polycarbonate (PC). The method consists of dipping polymer sheets in a solvent in which the polymer is partially soluble and then inducing solution crystallization by dipping the sheet in a poor solvent for several seconds. A solvent mixture of methyl ethyl ketone and isopropyl alcohol (IPA) was optimized to shorten the crystallization time in a poor solvent. Single-walled carbon nanotubes, multiwalled carbon nanotubes (MWNTs), and graphene sheets were used to nucleate PC crystallization. In particular, monolayer graphene sheets were prepared by reducing graphene oxide with hydrazine. Crystalline micro- and nanostructures rapidly formed upon dipping of the PC sheets in the solution containing NCs, followed by immersion in IPA. The structures depended on the dimensions of the NCs. Especially, in the MWNT solution, dipping for 10 s was sufficient to create a superhydrophobic surface. Crystallization of PC and the incorporation of NCs during crystallization were characterized by Raman spectroscopy.

KEYWORDS: carbon nanotubes • graphene • superhydrophobicity • polymer • crystallization

1. INTRODUCTION

Low-dimensional carbon materials (nanocarbons, NCs), such as one-dimensional (1D) carbon nanotubes (CNTs) and two-dimensional (2D) graphene sheets, have a strong ability to induce crystallization of polymers in composites and solutions (1−13). Structurally, CNTs and graphene sheets have the same primitive structural unit of graphite layers. However, the topological crystalline structures of polymers nucleated by these NCs can be affected by the dimensional differences between NCs. In dilute solutions and even melt systems, semicrystalline polymers form unique crystalline morphologies, such as a nanohybrid shish-kebab structure, in the presence of CNTs, which is considered as "soft epitaxy" (1−4).

Recently, crystalline polymers, such as polypropylene (PP) (14), polyethylene (PE) (15), polycarbonate (PC) (16), and poly(L-lactide) (17), were used to fabricate hierarchical superhydrophobic surfaces by solvent-induced crystallization. The superhydrophobic surfaces, with a water contact angle (CA) greater than 150° and a sliding angle less than 10°, have recently attracted significant attention because of their unique water-repellent and self-cleaning properties and their potential for practical applications ranging from biotechnology to self-cleaning commodity materials (18−28). However, until now no attempts have been made to minimize the fabrication time of superhydrophobic crystalline polymer surfaces by the addition of foreign materials. In pure polymer systems, deposited polymers act as nuclei around which the polymer-rich phase aggregates, thereby decreasing the system's surface tension. The effective nucleation abilities and unique morphological features of CNTs and graphene sheets therefore inspired us to accelerate the time required for solution crystallization of polymers in the fabrication of superhydrophobic surfaces.

In this communication, we present a facile method for the rapid creation of superhydrophobic surfaces via solution crystallization of amorphous PC in solvent mixtures assisted by low-dimensional NC materials such as CNTs and graphene sheets. We investigated the dimensional dependence of the resulting PC crystalline structure. To achieve this goal, first, the volume ratio of good and poor solvents was optimized to decrease the crystallization time for PC. The sequential dipping of polymer sheets in CNT or graphene solutions and in a poor solvent induced rapid formation of superhydrophobic surfaces with micro- and nanostructures via NC-induced crystallization of amorphous PC surfaces. The crystallization of PC and incorporation of NC materials into superhydrophobic surfaces were characterized by Raman spectroscopy.

2. EXPERIMENTAL METHODS

Single-walled carbon nanotubes (SWNTs), produced by the arc-discharge method (P3) and functionalized by HNO_3 treatment, were purchased from Carbon Solution Inc. and used as

* To whom correspondence should be addressed. Tel: +82-55-280-1678. Fax: +82-55-280-1590. E-mail: jthan@keri.re.kr (J.T.H.), gwleephd@keri.re.kr (G.-W.L.).

Received for review September 7, 2010 and accepted October 13, 2010

† Korea Electrotechnology Research Institute.

‡ Massachusetts Institute of Technology.

DOI: 10.1021/am1008425

Published on Web 10/28/2010

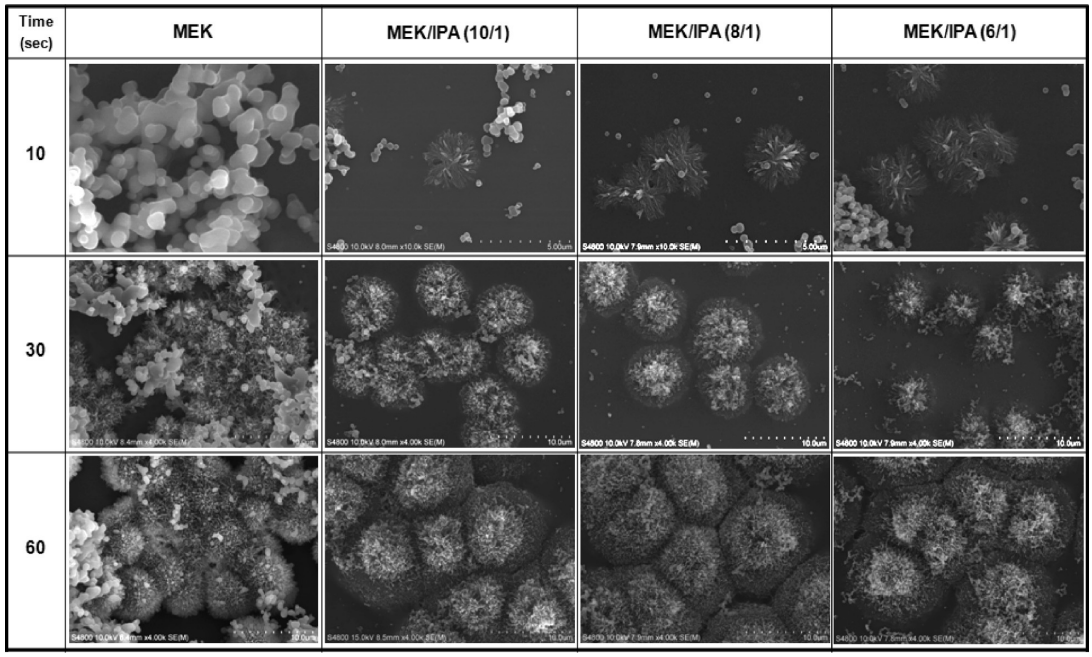

FIGURE 1. Scanning electron microscopy (SEM) images of PC surfaces after immersion in MEK, or the MEK/IPA solution, followed by dipping in IPA for several seconds.

received. Multiwalled carbon nanotubes (MWNTs) obtained from Iljin Nanotech Inc. were functionalized by an ultraviolet (UV)-ozone treatment for 1 h. Reduced graphene oxide (RGO) sheets were prepared by the reduction of graphene oxide (GO) with hydrazine at 80 °C for 24 h. Graphite oxide powder was synthesized by the Brodie method (29). Pure graphite (Alfa Aesar, 99.999% purity, −200 mesh) was mixed with fuming nitric acid and sodium chlorate at room temperature with stirring for 48 h. After acid treatment, the product was purified by washing, filtering, and cleaning. The amorphous PC sheets were obtained from i-Component Corp. and used as received. Methyl ethyl ketone (MEK) and isopropyl alcohol (IPA) were purchased from Aldrich and used as received. A total of 5 mg each of SWNTs, MWNTs, and RGO sheets were dispersed in 100 mL of MEK or MEK/IPA for 1 h in an ultrasonication bath. These solutions were diluted to investigate the effect of the NC concentration in solution on the crystallization of PC. PC sheets were dipped in pure MEK and in MEK/IPA solutions with different ratios or in NC solutions, and the sheets were subsequently immersed in IPA to coagulate or crystallize swollen PC.

Sample surface morphologies were analyzed using a scanning electron microscope (Hitachi S4800) and an optical microscope. The high-resolution Raman spectrometer (LabRAM HR800 UV) and transmission electron microscope (Hitachi 7600) were used to characterize the crystallization of PC and to confirm the existence of NCs in the crystalline structure. The water CAs were measured using a CA meter (Surfacetech Inc.).

3. RESULTS AND DISCUSSION

The fabrication method consists of dipping polymer sheets in a solvent in which the polymer was partially soluble, followed by polymer coagulation and crystallization induced by dipping in a poor solvent for several seconds. The crystallization of PC was controlled by varying the composition of the solvent solution, which changed the swelling volume. Solvents were selected based on the solubility parameters, boiling point, and miscibility of pairs of solvents. Volatile acetone and solvents with a high boiling point (bp), such as *N*,*N*-dimethylformamide or water, were excluded from the candidate solvents. MEK was used as the solvent. IPA was selected as the poor solvent because the swelling volume of PC in IPA is smaller than that in ethanol or methanol (30) and the bp of IPA is similar to that of MEK.

In general, a substance is soluble in a given solvent if the free energy of mixing, ΔG_{mix}, for the solute−solvent mixture is negative:

$$\Delta G_{mix} = \Delta H_{mix} - T\Delta S_{mix} \quad (1)$$

where ΔH_{mix} and ΔS_{mix} are the enthalpy and entropy of mixing, respectively, and T is the absolute temperature. For most system, ΔH_{mix} is a positive value, so that most solutions are driven by a large positive value of ΔS_{mix}. In this study, we modulated ΔS_{mix} by mixing MEK with IPA to control the solubility of PC in the solvent mixture. The molecular-level interactions between a solvent and another material include a combination of dispersive, polar, and hydrogen-bond interactions. Hansen proposed that the cohesive energy density of any materials is the sum of the dispersive, polar, and hydrogen-bonding components (31). The fractional parameter of the Hansen parameters for the solvents used in this study are shown in Figure S1 in the Supporting Information. Because crystallization of PC occurred by coagulation in a poor solvent, the crystallization rate of swollen PC is affected by the solubility and swelling volume of the PC surface layer, which depends on the solubility parameters and immersion time.

To optimize the solubility of PC in the dipping solution used for crystallization, the ratio between MEK and IPA was changed from 1:0 to 6:1 by volume. Superhydrophobic surfaces were fabricated by immersion of PC sheets into an MEK/IPA mixture, followed by dipping in IPA. The transparent sheet became opaque as a result of crystallization. As

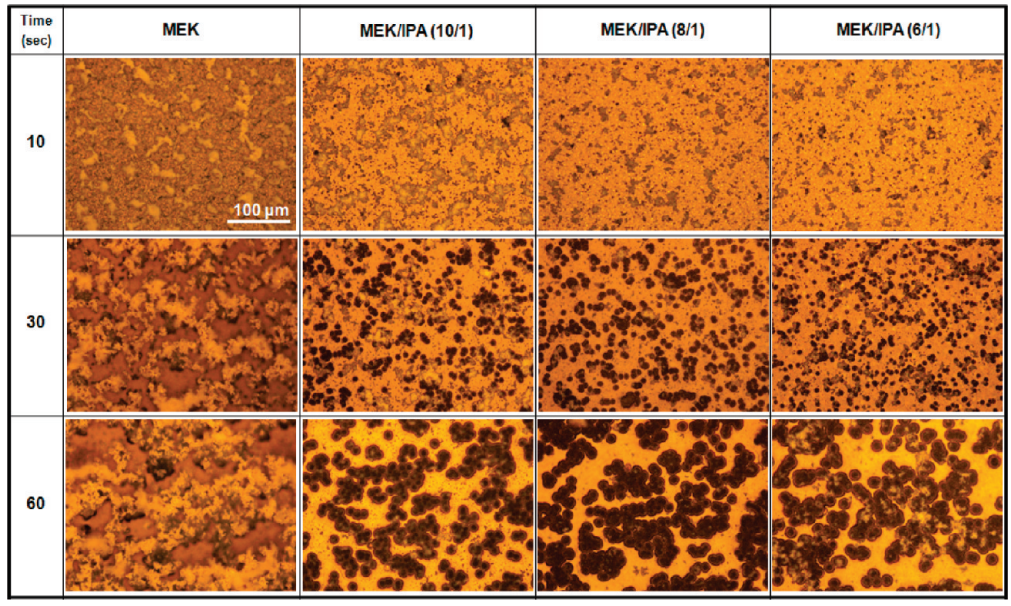

FIGURE 2. Optical microscopy images of PC sheets after immersion in MEK, or the MEK/IPA solution, followed by dipping in IPA for several seconds.

shown in Figure 1, dipping in pure MEK for 10 s did not produce a crystalline structure because the thin surface layer is dissolved well. Therefore, the polymer did not swell in MEK, and subsequent dipping in the poor solvent produced granular coagulation. Longer immersion times in MEK led to swelling of the PC surface, which resulted in the formation of a crystalline structure after dipping in the poor solvent. We modulated the solubility parameter of MEK by the addition of IPA to swell the surface layer of PC, which could be crystallized in the poor solvent. As shown in Figure 1, the addition of a poor solvent, IPA, accelerated the crystallization of PC even after dipping for 10 s because the surface layer swelled in the MEK/IPA mixture, in contrast with the behavior in the pure MEK. We note that a lotus leaflike structure (a natural self-cleaning surface morphology) was easily fabricated by dipping in the MEK/IPA solution for only 60 s. Optical microscopy images in Figure 2 showed that the 8:1 mixture of MEK and IPA was optimal for the fabrication of uniform microstructured surfaces after dipping for 60 s. By modulation of the solubility parameters for the solvent mixture, the crystallization time required for the formation of superhydrophobic surfaces was reduced. The CA increased to 160 ± 2° with the formation of micro- and nanostructured surfaces, whereas the smooth amorphous PC had a CA of only 79 ± 1°. This topological effect on the superhydrophobicity corresponds well to the Wenzel and Cassie–Boxter models (32, 33).

To further decrease the crystallization time for the rapid fabrication of superhydrophobic surfaces, we added SWNTs, MWNTs, and RGO sheets to the MEK/IPA (8:1) solution as heterogeneous nucleation agents. The diameters of bundled SWNTs and MWNTs were about 10 and 30 nm, respectively, as shown in Figure 3A,B. The SWNTs acted as a straight linear 1D structure, whereas the MWNTs showed a coiled structure. RGO sheets were synthesized via the hydrazine reduction of expanded graphite oxide by Brodie's method

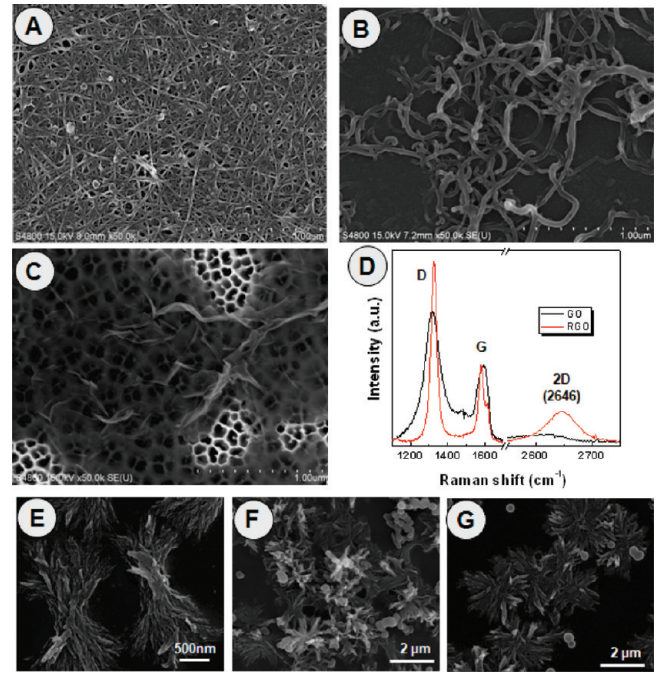

FIGURE 3. SEM images of (A) SWNTs, (B) MWNTs on silicon wafers, and (C) RGO sheets on an aluminum oxide membrane. (D) Raman spectra of GO and RGO sheets. (E–G) SEM images of PC surfaces after immersion in a MEK/IPA mixture solution containing SWNTs, MWNTs, and RGO sheets, respectively.

(29). The size of the 2D RGO sheets ranged from several micrometers to several tens of micrometers (Figure 3C). The second-order zone boundary phonon (2D) peaks at 2649 cm^{-1}, with a symmetric line shape in the Raman spectrum of RGO (Figure 3D), indicated a single-layered graphene sheet. The NCs were dispersed in the MEK/IPA (8:1 volume ratio) solution by bath sonication at a concentration of 20 mg/L for 1 h. PC sheets were then immersed into the NC solutions, followed by dipping in IPA. Parts E–G of Figure 3 show the surface morphologies of PC sheets after dipping

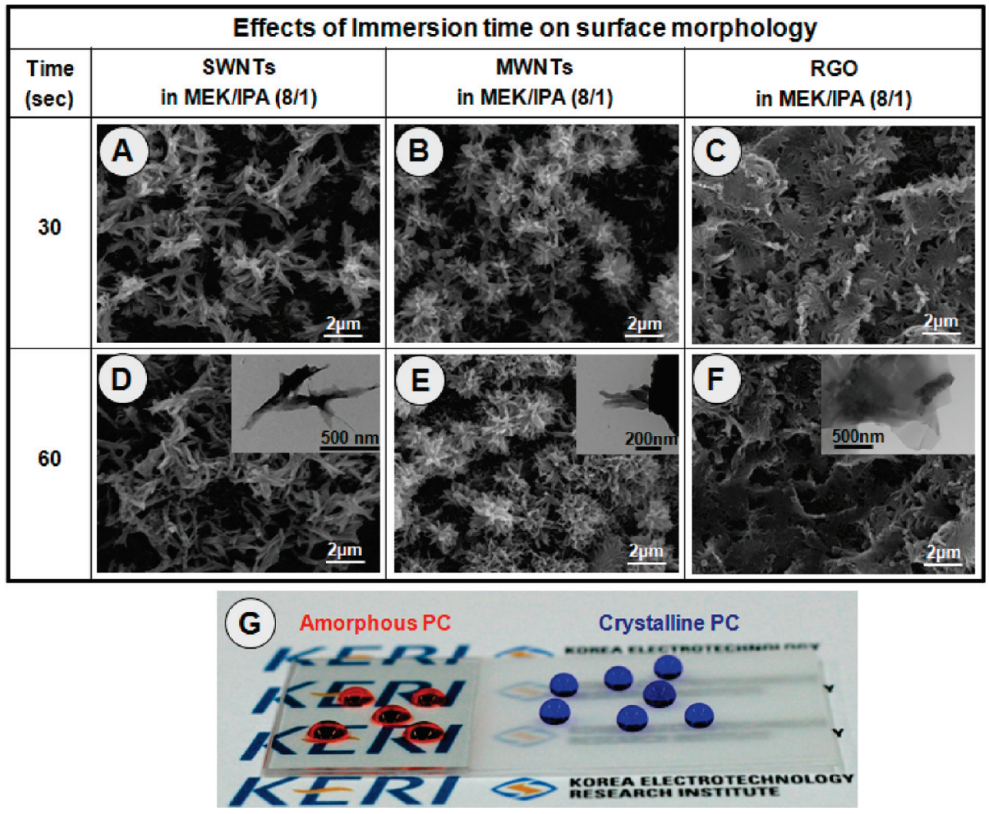

FIGURE 4. (A−F) SEM images of PC surfaces after immersion in the MEK/IPA solution containing 20 mg/L NCs for different periods of time. Insets in D−F: TEM image of NCs incorporated in the crystalline PC structures. The optical image in part G shows ink droplets on an amorphous PC surface (left) and on an NC-induced crystalline PC surface (right).

in the NC solutions for 10 s. Interestingly, 10 s of dipping in NC solutions produced crystallized PC shapes that depended on the dimensions of the NCs. We note that the shape of the crystallized PC became anisotropic in the presence of SWNTs because of the incorporation of anisotropic 1D SWNTs having bundle diameters and lengths of about 10 nm and several micrometers, respectively. MWNTs of 30 nm diameter produced flowerlike crystalline structures even with dipping for 10 s. These structures may possibly have been due to the coiled structure of the MWNTs, and the density of these structures increased upon the addition of more MWNTs without changes in shape. In the case of 2D RGO, a flat-flowerlike crystalline structure was formed upon dipping for 10 s, whereas the highly oxidized GOs were not effective nucleation agents, as shown in Figure S2 in the Supporting Information. These results indicated that PC crystals grown in the presence of NCs nucleated via a heterogeneous nucleation mechanism. The growth mechanism involved the cooperative orientation of the polymer chains and the NC surfaces, and it was dimension-dependent. A typical polymer possesses a radius of gyration of ~10 nm. Thus, the bundled SWNTs ~10 nm in size may form a shish layer on the SWNT surface, yielding an anisotropic macrostructure. Coiled MWNTs, characterized by diameters that are several tens of nanometers, present multiple nucleation sites to produce flowerlike microstructures. The flat-flowerlike structure in Figure 3G arose in the presence of the 2D structure of the RGO sheets. Thus, the crystalline granule size was larger than that produced in the nanotube solution. These results indicated that the size of the crystalline structure depended heavily on the dimensions of the NC materials. Note that dipping for only 10 s in a 10 mg/L MWNT solution was sufficient to produce micro- and nanostructured superhydrophobic surfaces with a CA of 165 ± 3°, which shows very low CA hysteresis (<5°). However, measurements of the surface superhydrophobicity suggested that 10 s of dipping in SWNTs or RGO solutions produced a surface roughness that was insufficient to yield a superhydrophobic state, and more dipping time needs to satisfy enough of the superhydrophobic crystalline structure. These suggest that the coiled MWNTs were more effective nucleation agents than SWNTs or RGO sheets in terms of structuring the PC during solution crystallization. The effects of the NC concentration on the crystalline structures of PC were more clarified by increased immersion time, as shown in Figure S3 in the Supporting Information.

Figure 4 shows the surface morphologies of the PC sheets as a function of the immersion time in a solution containing 20 mg/L SWNTs, MWNTs, or RGO sheets. We note that 30 s of dipping time in NC solutions was sufficient for the fabrication of superhydrophobic surfaces showing high water CAs exceeding 160°, as shown in Figure 4G. The SWNT solution yielded a more anisotropic crystalline structure after 60 s of immersion because of the incorporation of additional SWNTs. Upon dipping in the MWNT solutions, the flowerlike crystalline structures of PC remained constant in size, and only the number density of the structures increased upon an increase in the dipping time. More

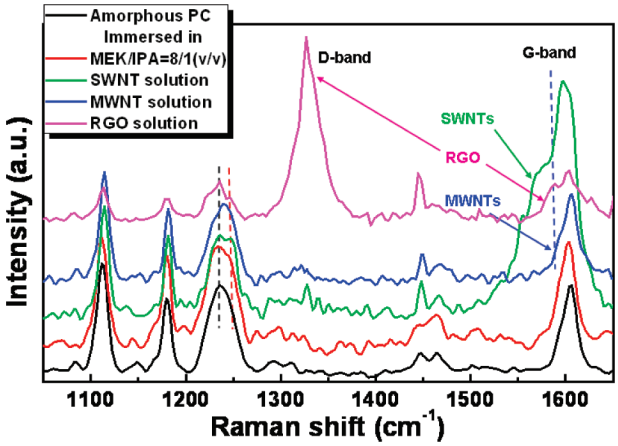

FIGURE 5. Raman spectra excited at 633 nm of amorphous PC and PC samples immersed in the MEK/IPA (8:1) solution or solutions with SWNTs, MWNTs, and RGO sheets. Dotted black and red lines indicate the C−O−C stretching mode of amorphous and crystalline PC, respectively. The dotted blue line indicates the G band from the NCs.

extensive 2D-like crystalline structures were formed by dipping in the 2D RGO solution for 60 s. Transmission electron microscopy (TEM) images in the insets of Figure 4D−F clearly reveal the existence of NCs in the crystalline PC structure. The CA hysteresis did not exceed 5° because of the well-developed micro- and nanostructures over the area. By dipping in the NC solution, we produced a superhydrophobic tray, as shown in Figure S4 in the Supporting Information. Using this tray, we easily observed deformation of a water droplet on the superhydrophobic surfaces.

Conformational structures and intermolecular arrangements of the amorphous and semicrystalline PC samples were characterized by Raman spectroscopy measurements (34). Raman spectroscopy is also a useful tool for obtaining the phonon spectrum of NC materials (35, 36). Crystallization of PC and the incorporation of NCs during nucleated crystallization were investigated by Raman spectroscopy. Figure 5 shows the Raman spectra of amorphous PC and PCs immersed in a MEK/IPA (8:1) mixture or NC solutions. The transition from amorphous to crystalline PC was observed in a region corresponding to the stretching vibration of the C−O−C group (34). As shown in Figure 5, the band at 1235 cm^{-1} from the C−O−C group of amorphous PC was shifted to 1248 cm^{-1} with shoulders at 1237 and 1220 cm^{-1} after dipping in the MEK/IPA mixture and NC solutions. This observation indicated that the amorphous PC crystallized upon sequential dipping in the MEK/IPA solution and IPA. Moreover, the incorporation of NCs during crystallization of PC in solution was confirmed by the presence of the G-band peaks below 1580 cm^{-1} and a D-band peak at 1350 cm^{-1}, both because of the nanotubes and RGO sheets. Therefore, the NC materials were excellent heterogeneous nucleating agents for solution crystallization of PC, resulting in a rapid transformation of the PC surfaces into superhydrophobic surfaces.

4. CONCLUSIONS

We reported a facile method for fabricating superhydrophobic crystalline polymer surfaces by solubility modulation and NC-induced crystallization of PC. NC materials such as SWNTs, MWNTs, and RGO sheets were used to nucleate PC crystallization. The solution crystallization of PC was performed by dipping polymer sheets in a partial solvent containing the NCs and poor solvent, sequentially. It was found that the size and shape of the crystalline structures depend on the dimensions of the NCs. In particular, dipping for only 10 s in a MWNT solution produced superhydrophobic surfaces with low CA hysteresis. The crystallization of PC and the incorporation of NCs during crystallization were characterized by Raman spectroscopy and TEM.

Acknowledgment. This work was supported by grants from the Fundamental R&D Program for Core Technology of Materials funded by the Ministry of Knowledge Economy and from KERI (Grant 10-12-N0101-17), Republic of Korea. We also thank to S. G. Lee at POSTECH for the experimental assistance.

Supporting Information Available: Geometric graph of the Hansen solubility parameter for solvents and SEM images of PC surfaces after immersion in a MEK/IPA solution containing NCs and GO. This material is available free of charge via the Internet at http://pubs.acs.org.

REFERENCES AND NOTES

(1) Li, C. Y.; Li, L. Y.; Cai, W. W.; Kodjie, S. L.; Tenneti, K. K. *Adv. Mater.* **2005**, *17*, 1198.
(2) Li, L.; Li, C. Y.; Ni, C. *J. Am. Chem. Soc.* **2006**, *128*, 1692.
(3) Li, L. Y.; Yang, Y.; Yang, G. L.; Chen, X. M.; Hsiao, B. S.; Chu, B.; Spanier, J. E.; Li, C. Y. *Nano Lett.* **2006**, *6*, 1007.
(4) Yang, J. H.; Wang, C. Y.; Wang, K.; Zhang, Q.; Chen, F.; Du, R. N.; Fu, Q. *Macromolecules* **2009**, *42*, 7016.
(5) Wang, W.; Xie, X.; Ye, X. *Carbon* **2010**, *48*, 1670.
(6) Grady, B. P.; Pompeo, F.; Shambaugh, R. L.; Resasco, D. E. *J. Phys. Chem. B* **2002**, *106*, 5852.
(7) Yang, X.; Li, L.; Shang, S.; Tao, X. *Polymer* **2010**, *51*, 3431.
(8) Xu, J.-Z.; Chen, T.; Yang, C.-L.; Li, Z.-M.; Mao, Y.-M.; Zeng, B.-Q.; Hsiao, B. S. *Macromolecules* **2010**, *43*, 5000.
(9) Lu, K. B.; Grossiord, N.; Koning, C. E.; Miltner, H. E.; van Mele, B.; Loos, J. *Macromolecules* **2008**, *41*, 8081.
(10) Haggenmueller, R.; Fischer, J. E.; Winey, K. I. *Macromolecules* **2006**, *39*, 2964.
(11) Anand, K. A.; Agarwal, U. S.; Joseph, R. *Polymer* **2006**, *47*, 3976.
(12) Moniruzzaman, M.; Winey, K. I. *Macromolecules* **2006**, *39*, 5194.
(13) Sung, Y. T.; Kum, C. K.; Lee, H. S.; Byon, N. S.; Yoon, H. G.; Kim, W. N. *Polymer* **2005**, *46*, 5656.
(14) Erbil, H. Y.; Demirel, A. L.; Avcı, Y.; Mert, O. *Science* **2003**, *299*, 1377.
(15) Lu, X.; Zhang, C.; Han, Y. *Macromol. Rapid Commun.* **2004**, *25*, 1606.
(16) Zhao, N.; Xu, J.; Xie, Q.; Weng, L.; Guo, X.; Zhang, X.; Shi, L. *Macromol. Rapid Commun.* **2005**, *26*, 1075.
(17) Song, W.; Veiga, D. D.; Custódio, C. A.; Mano, J. F. *Adv. Mater.* **2009**, *21*, 1830.
(18) Barthlott, W.; Neinhuis, C. *Planta* **1997**, *202*, 1.
(19) Oner, D.; McCarthy, T. *Langmuir* **2000**, *16*, 7777.
(20) Feng, L.; Li, S.; Li, Y.; Li, H.; Zhang, L.; Zhai, J.; Song, Y.; Liu, B.; Jiang, L.; Zhu, D. *Adv. Mater.* **2002**, *14*, 1857.
(21) Genzer, J.; Efimenko, K. *Biofouling* **2006**, *22*, 339.
(22) Lafuma, A.; Quéré, D. *Nat. Mater.* **2003**, *2*, 457.
(23) Marmur, A. *Langmuir* **2004**, *20*, 3517.
(24) Zhai, L.; Cebeci, F. Ç.; Cohen, R. E.; Rubner, M. F. *Nano Lett.* **2004**, *4*, 1349.
(25) Jiang, L.; Zhao, Y.; Zhai, J. *Angew. Chem., Int. Ed.* **2004**, *43*, 4338.

(26) Han, J. T.; Lee, D. H.; Ryu, C. Y.; Cho, K. *J. Am. Chem. Soc.* **2004**, *126*, 4796.
(27) Han, J. T.; Kim, S.; Karim, A. *Langmuir* **2007**, *23*, 2608.
(28) Han, J. T.; Kim, S. Y.; Woo, J. S.; Lee, G.-W. *Adv. Mater.* **2008**, *20*, 3724.
(29) Brodie, B. C. *Ann. Chim. Phys.* **1860**, *59*, 466.
(30) Kambour, R. P.; Gruner, C. L.; Romagosa, E. E. *Macromolecules* **1974**, *7*, 248.
(31) Hansen, C. M. *Hansen Solubility Parameters, A User's Handbook*; CRC Press: Boca Raton, FL, 2007.
(32) Wenzel, R. N. *Ind. Eng. Chem.* **1936**, *28*, 988.
(33) Cassie, A. B. D.; Baxter, S. *Trans. Faraday Soc.* **1944**, *40*, 546.
(34) Dybal, J.; Schmidt, P.; Baldrian, J.; Kratochvíl, J. *Macromolecules* **1998**, *31*, 6611.
(35) Jorio, A.; Pimenta, M. A.; Souza Filho, A. G.; Saito, R.; Dresselhaus, G.; Dresselhaus, M. S. *New J. Phys.* **2003**, *5*, 139–141.
(36) Ferrari, A. C.; Meyer, J. C.; Scardaci, V.; Casiraghi, C.; Lazzeri, M.; Mauri, F.; Piscanec, S.; Jiang, D.; Novoselov, K. S.; Roth, S.; Geim, A. K. *Phys. Rev. Lett.* **2006**, *97*, 187401.

AM1008425